

STRUCTURAL AND PHASE STATE OF CERAMICS BASED ON SILICON CARBIDE IRRADIATED WITH HIGH ENERGY KRYPTON AND XENON IONS

V.V. Uglov,^{1,*} P.S. Grinchuk,² M.V. Kiyashko,² V.M. Kholad,¹
S.V. Zlotski,¹ V.A. Skuratov,³ & A. Issatov³

¹Belarusian State University, Minsk, 220030, Belarus

²A.V. Luikov Institute of Heat and Mass Transfer of the National Academy of Science of Belarus, Minsk 220072, Belarus

³Joint Institute for Nuclear Research, Moscow Region, 141980 Dubna, Russia

*Address all correspondence to: V.V. Uglov, Belarusian State University, 4 Nezavisimosty Ave., Minsk, 220030, Belarus; Tel.: +375172096257, E-mail: Uglov@bsu.by

Original Manuscript Submitted: 3/22/2022; Final Draft Received: 3/22/2022

The effect of high-energy irradiation with Kr (107 MeV) and Xe (167 MeV) ions with fluence up to 5×10^{13} was studied. The samples showed radiation resistance of the phase composition to irradiation. Irradiation leads to deformation of the crystal lattice. The value of deformation under irradiation with Xe ions is 1.1 times greater for parameter a and 1.3 times for parameter c than with Kr ions, which is due to the high damaging ability of Xe ions.

KEY WORDS: silicon carbide, 6H-SiC, Kr, Xe

1. INTRODUCTION

Due to its superior high-temperature strength, high thermal conductivity, chemical inertness, and small neutron capture cross section, silicon carbide (SiC) is suitable for use as structural components in nuclear fusion reactors, or as an encapsulating material for nuclear fuel in light water reactors and gas-cooled fission reactors, and also in radioactive nuclear waste disposals. Thus, the study of the radiation resistance of the structural-phase state and the nature of the evolution of defects in silicon carbide after simulated ion irradiation of fission fragments is a relevant task (Xu et al., 2012).

2. MATERIALS AND EXPERIMENTAL DETAILS

The samples were prepared at the Lykov Institute of Heat and Mass Transfer. The main stages of the preparation of reaction-bound Si/SiC ceramics are schematically shown in Fig. 1.

Two commercially available fractions of silicon carbide powder were used as raw material: coarse M50 grade with characteristic grain size of 50 μm and fine M5 grade with grain size of 5 μm (Volzhsky Abrasive Works, Russia). The ratio of large and small fractions was 5:3. Silicon carbide powder (88 wt.%) was mixed with a thermoplastic binder based on paraffin P-2 (12 wt.%) and was cast into the mold. Thermal removal of the binder was carried out in air at 600°C. Bakelite varnish based on resole resins LBS-1 (plant named after Yu.M. Sverdlov, Russia) was

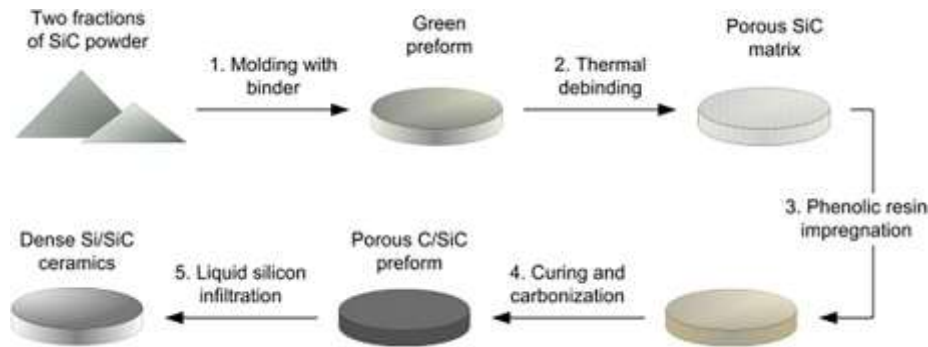


FIG. 1: The main stages of the preparation of SiC ceramics

used for impregnation of a porous SiC matrix after removal of the binder. The impregnation temperature was 40°C, the pressure was 0.5 MPa. After the impregnation stage, the workpiece was dried in the air at 160°C for 4 hours. Then the workpiece was subjected to pyrolysis in a vacuum furnace (VacETO, Russia) at a temperature of 1200°C and a pressure of 0.13 Pa for 2 hours.

The same vacuum furnace was used for the final siliconizing stage, which was carried out at a temperature of 1800°C and a pressure of 0.13 Pa for 4 hours. For this purpose, the sample was placed in a closed graphite crucible and covered with a homogeneous layer of electronic purity silicon powder (Semiconductor Plant, Ukraine), which melted when heated and penetrated into the porous structure of the C/SiC workpiece. A chemical reaction took place between liquid silicon and carbon in the pores with the formation of secondary silicon carbide, which bound the initial particles of primary silicon carbide powders. The remaining space remained filled with silicon. After siliconizing, the sample surface became rough and inhomogeneous, so mechanical grinding and polishing were used to remove residual silicon and create appropriate conditions for further study of ceramics (Grinchuk et al., 2018).

The analysis of the obtained samples of silicon carbide ceramics showed that it contains about 78% of silicon carbide and less than 2% of single residual pores with a characteristic size of up to several microns. Figure 2 shows a micrograph of the sample section from an optical microscope. Dark areas correspond to silicon carbide, light areas correspond to silicon.

The samples were irradiated with Kr ions with an energy of 107 MeV and Xe ions with an energy of 167 MeV at room temperature at the IC-100 linear heavy ion accelerator at JINR (Dubna, Russia). The integral radiation doses were: 1×10^{12} , 1×10^{13} cm⁻² for krypton, and 1×10^{12} , 1×10^{13} , 5×10^{13} sm⁻² for xenon.

The structural and phase state of the initial and irradiated silicon carbide samples was studied by X-ray diffraction analysis (XRD) and Raman scattering (Raman). X-ray analysis was performed on an Ultima IV diffractometer using the geometry of a parallel beam in copper (CuK α) radiation with a wavelength of 0.154179 nm. The Raman was carried out at room temperature using a spectral-analytical complex based on a scanning confocal microscope “Nanofinder High-End.” The excitation wavelength was 532 nm, and the excitation depth exceeded 10 microns.

3. RESULT AND DISCUSSIONS

Figure 3 shows an X-ray image of an unirradiated silicon carbide sample. Studies of the phase composition showed that the initial samples are a multiphase system: SiC-6H: hexagonal (P63mc) syngony, Si: cubic (Fd-3m) syngony, SiC-15R: trigonal (R3m) syngony, and FeSi₂: tetragonal (P4/mmm) syngony (Fig. 3). The main phase is SiC-6H (about 80%), the content of the SiC-15R phase is about 10%, Si is less than 8%, and FeSi₂ is less than 2%.

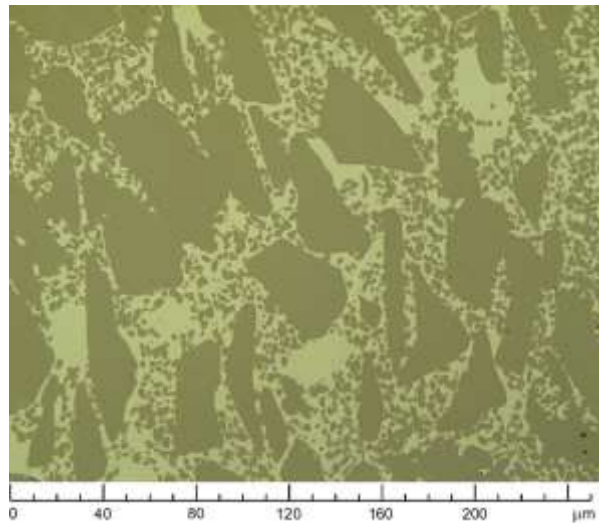


FIG. 2: The section of reaction-bound ceramics. Optical microscope, reflected light, $50 \times$ lens

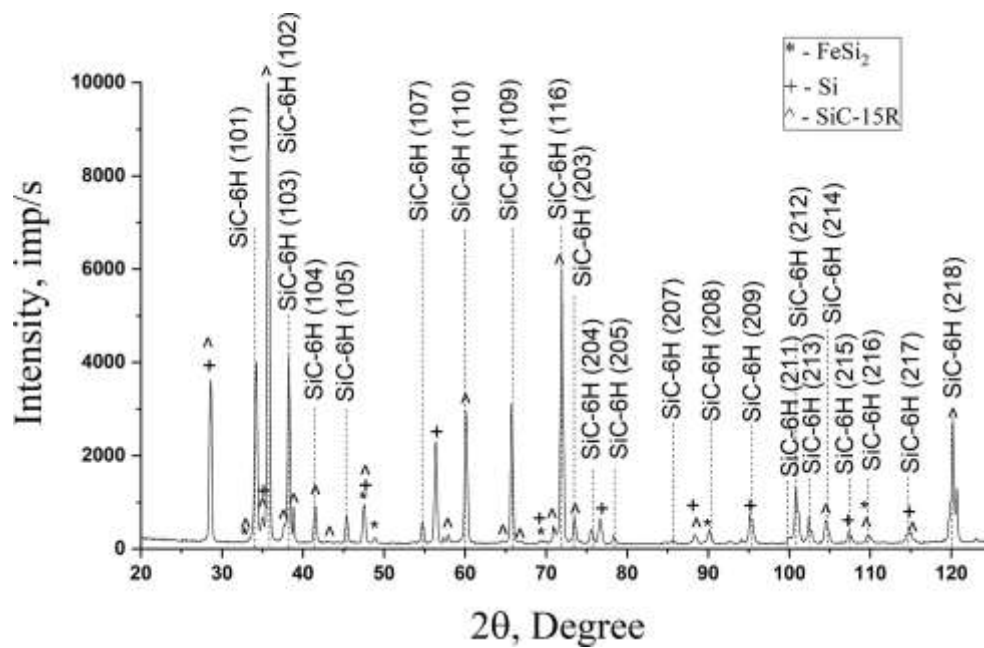


FIG. 3: XRD of the initial SiC sample

Figure 4 shows the results of modeling the irradiation of silicon carbide samples in the stopping and range of ions in matter (SRIM). SRIM calculations showed that the projective range of Kr and Xe ions are 12.4 and 13.9 microns, the maximum energy losses for ionization in the near-surface region are 12 and 18 keV/nm, and the maximum of the vacancy distribution corresponds to 12 and 18 vacancies/(nm³ion), respectively.

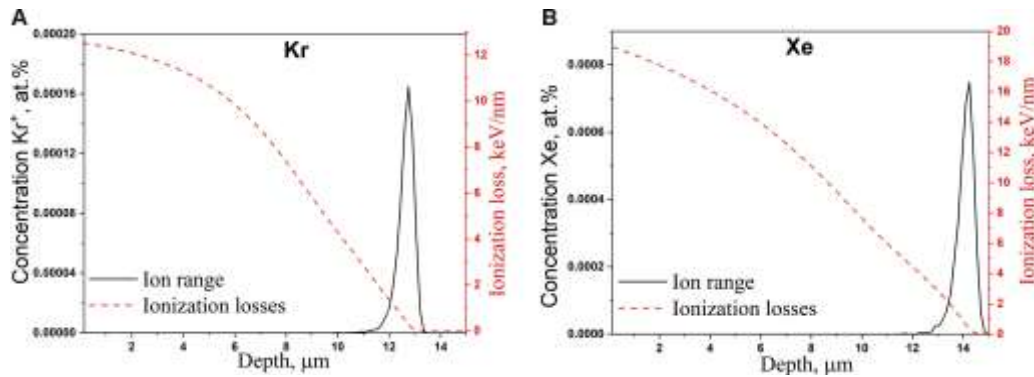


FIG. 4: Simulation results of irradiation of SiC samples with Kr (a) and Xe (b) ions in SRIM

The X-ray analysis of samples after irradiation with Kr and Xe ions showed high radiation resistance of the phase composition when irradiated with Kr (107 MeV) and Xe (167 MeV) ions with doses up to $5 \times 10^{13} \text{ cm}^{-2}$. The decay of existing phases or the formation of new ones was not observed. Irradiation with Kr and Xe ions leads only to a change in the crystal lattice parameter of the phases of silicon carbide samples.

Figure 5 shows the dependence of the relative change of lattice parameters ($\Delta c/c_0$) and ($\Delta a/a_0$) on the dose of krypton and xenon ions irradiation. The lattice parameters a and c were calculated using the Rietveld method. The lattice parameters of the unirradiated SiC-6H were used as a_0 and c_0 . The relative change in the lattice parameters a and c are associated with the deformation of the lattice.

It is seen that irradiation with high-energy Kr and Xe ions leads to a significant increase in lattice deformation (compressive stresses), which is due to the formation of radiation defects and their clusters (Singh et al., 2019). With a further increase in the dose of Kr ion irradiation to $1 \times 10^{13} \text{ cm}^{-2}$, the lattice deformations ($(c-c_0)/c_0$) does not change and ($(a-a_0)/a_0$) increases slightly. With an increase in the dose of Xe ion irradiation to $1 \times 10^{13} \text{ cm}^{-2}$ and $5 \times 10^{13} \text{ cm}^{-2}$, the lattice deformations ($(c-c_0)/c_0$) and ($(a-a_0)/a_0$) increase with increasing dose, which is due to an increase

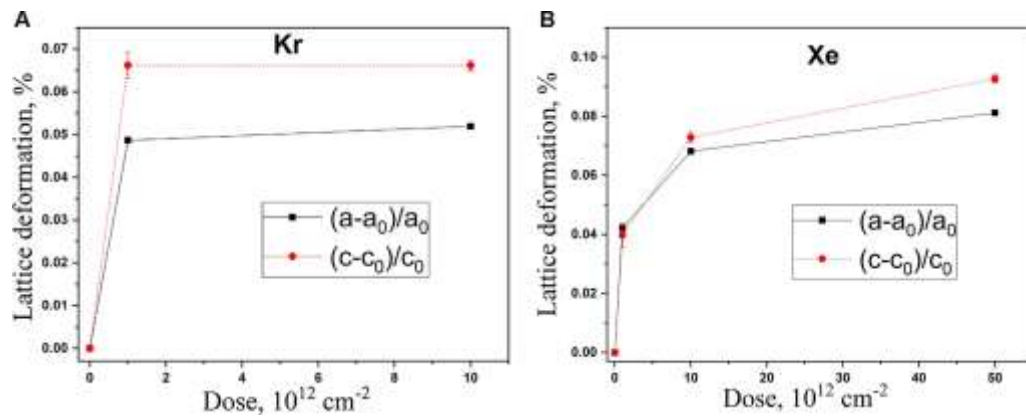


FIG. 5: Dependence of lattice deformations $(a-a_0)/a_0$ and $(c-c_0)/c_0$ (for 6H-SiC) at different doses of SiC irradiated with Kr (a) and Xe (b) ions

in the degree of overlap of ion tracks and an increase in the number of radiation defects. It is also seen that after irradiation with Xe ions, the values of deformations $((a-a_0)/a_0)$ and $((c-c_0)/c_0)$ are 1.3 and 1.1 times higher, respectively, than with Kr ions at a dose of $1 \times 10^{13} \text{ cm}^{-2}$ (Zikirina et al., 2021). Large values of deformations during irradiation with Xe ions are due to their higher damaging ability (formation of vacancies, energy losses for ionization). The obtained data on the deformation of the lattice are averaged over the depth of implantation.

Figure 6 shows the Raman scattering spectra for silicon carbide samples irradiated with Kr and Xe ions. For the convenience of comparison, the spectra are shown on the same graph.

As a wurtzite structure, the 6H-SiC phase has active phonon combination modes, which can be divided into longitudinal (LO) and transverse (TO): A_1 (LO), E_1 (TO) and E_2 (TO).

Four peaks of the first order of Si-C oscillations were detected in SiC samples at approximately 766 , 788 , 796 , and 966 cm^{-1} , corresponding to the modes E_2 (TO), E_1 (TO), E_2 (TO), and A_1 (LO), respectively (Chen et al., 2016). The mode E_2 (TO) (766 cm^{-1}) corresponds to disordered Si-C bonds (Fig. 6).

Ion irradiation leads to a slight decrease in the intensity of Si-C peaks and an increase in their full width at half maximum. This is due to the formation and accumulation of radiation defects in the SiC sample (Xu et al., 2018). Figure 6 also shows a clear shift of the lines E_1 (TO) and E_2 (TO) to the region of the Raman shift reduction, which indicates the occurrence of positive deformations, which correspond to the deformation $\Delta a/a_0$. For the peaks A_1 (LO), which correspond to the deformation $((c-c_0)/c_0)$, its displacement to the region of decreasing Raman shift is also visible.

4. CONCLUSION

Samples of silicon carbide ceramics representing a multiphase system are synthesized: SiC-6H, Si, SiC-15R, and FeSi_2 . The main phase is SiC-6H (~ 80%).

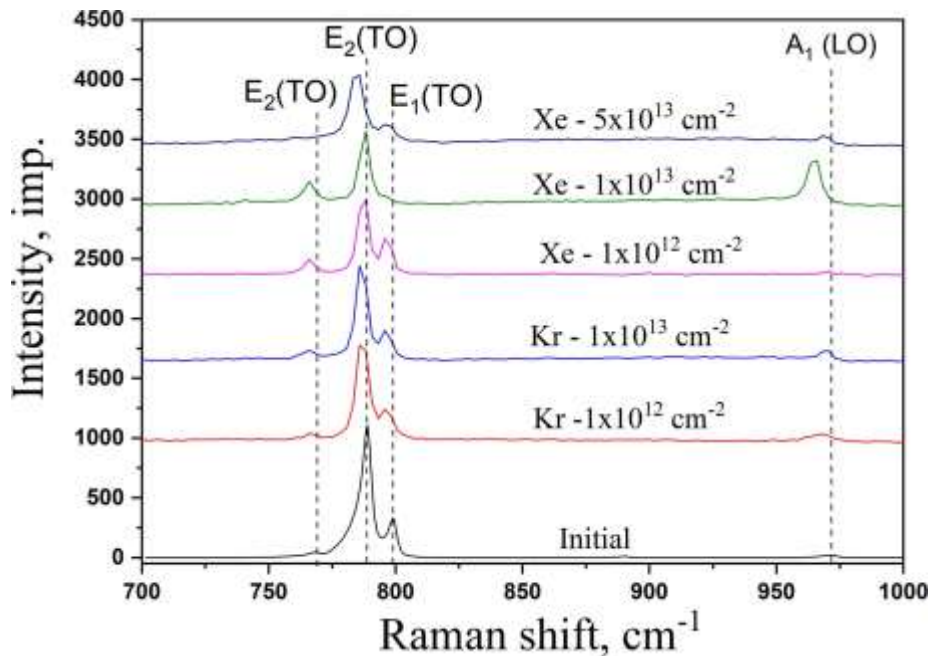


FIG. 6: Raman scattering spectrum of the initial and irradiated SiC samples

Stability of structural parameters is observed in the samples, which indicates radiation resistance of silicon carbide samples upon irradiation with high-energy Kr (107 MeV) and Xe (167 MeV) ions with doses up to $5 \times 10^{13} \text{ cm}^{-2}$.

It was found that irradiation with Kr and Xe ions leads to a significant increase in lattice deformation in SiC-6H, and the level of deformations increases during the transition from Kr ions to Xe ions.

The Raman method revealed a shift and a change in the shape of peaks corresponding to Si-C bonds, which is associated with the occurrence of deformations in the SiC-6H structure after ion irradiation. It can also be noted that the results of studies using X-ray diffraction analysis and Raman scattering methods are in good agreement with each other and complement each other.

The conducted studies of irradiated silicon carbide samples allow us to conclude that the SiC-6H phase has a high radiation resistance to high-energy irradiation with heavy ions.

REFERENCES

- Chen, X., Zhou, W., Feng, Q., Zheng, J., Liu, X., Tang, B., Xue, J., and Peng, S., Irradiation Effects in 6He-SiC Induced by Neutron and Heavy Ions: Raman Spectroscopy and High-Resolution XRD Analysis, *J. Nucl. Mater.*, vol. **478**, pp. 215–221, 2016.
- Grinchuk, P.S., Kiyashko, M.V., Abuhimd, H.M., Alshahrani, M.S., Stepkin, M.O., Toropov, V.V., Khort, A.A., Solovei, D.V., Akulich, A.V., Shashkov, M.D., and Liakh, M.Yu., Effect of Technological Parameters on Densification of Reaction Bonded Si/SiC Ceramics, *J. Eur. Ceram. Soc.*, vol. **38**, pp. 4815–4823, 2018.
- Singh, F., Rawat, M., Gautam, S.K., and Ojha, S., Micro-Raman Investigations on Zirconium Oxidefilm During Swift Heavy Ion Irradiation to Study Crystalline-to-Crystalline Phase Transformation Kinetics by Cascade Overlap Model, *J. Appl. Phys.*, vol. **126**, Article ID 025901, 2019.
- Xu, Z., He, Z., Song, Y., Fu, X., Rommel, M., Luo, X., Hartmaier, A., Zhang, J., and Fang, F., Topic Review: Application of Raman Spectroscopy Characterization in Micro/Nano-Machining, *Micromachines*, vol. **9**, 361, 2018.
- Xu, C.L., Zhang, C.H., Li, J.J., Zhang, L.Q., Yang, Y.T., Song, Y., Jia, X.J., Li, J.Y., and Chen, K.Q., A HRXRD and Nano-Indentation Study on Ne-Implanted 6H-SiC, *Nucl. Inst. Methods Phys. Res.*, vol. **286**, pp. 129–133, 2012.
- Zikirina, A., Kadyrzhanov, K.K., Kenzhina, I.E., Kozlovskiy, A.L., and Zdorovets, M.V., Study of Defect Formation Processes under Heavy Ion Irradiation of ZnCo₂O₄ Nanowires, *Opt. Mater.*, vol. **118**, Article ID 111282, 2021.